

Microarray expression profile and bioinformatic analyses of circular RNA in human esophageal carcinoma

Xiaohua Chen (✉ cxh0663@126.com)

Guangzhou Panyu Central Hospital <https://orcid.org/0000-0001-7536-5061>

Liping Wang

The first city hospital of Chenzhou

Sina Cai

The third affiliated hospital of Nanfang Medical University

Xiaona Zhang

Sun Yat-sen University Sixth Affiliated Hospital

Wenhui Li

Guangzhou Panyu Central Hospital

Henglun Liang

Guangzhou Panyu Central Hospital

Research article

Keywords: esophageal carcinoma, circular RNAs, microarray, microRNA sponge, bioinformatic analyze

Posted Date: September 18th, 2019

DOI: <https://doi.org/10.21203/rs.2.14623/v1>

License: © ⓘ This work is licensed under a Creative Commons Attribution 4.0 International License. [Read Full License](#)

Abstract

Background : Recent studies indicate that noncoding circular RNAs (circRNAs) are involved in the development of esophageal carcinoma. This study aimed to identify circRNAs that are differentially expressed in esophageal carcinoma (EC), which may provide potential biomarkers and therapeutic targets for EC and improve the understanding of its tumorigenesis mechanism.

Methods : Ten samples of esophageal carcinoma tissues were sent for circRNA microarray detection. Then the data was subjected to bioinformatic analysis (including circRNA-miRNA (miRNA) coexpression network, Spearman's correlation test and cancer-related circRNA-miRNA axis analyses). The gene expressions of key circRNAs were detected by real-time-PCR.

Results: A total of 102 upregulated and 67 significantly downregulated circRNAs were identified in EC tumors compared to adjacent normal tissue by microarray analysis. One upregulated circRNA (hsa_circRNA_401955) showed the most correlation and was thus regarded as the hub gene by the Spearman correlation test. KEGG pathway enrichment analyses showed that four primary pathways (mRNA surveillance, cytoskeleton actin regulation, spliceosome and the NOD-like receptor signaling pathway) were predicted in the five connected miRNA response elements (MREs) of hub circRNA's. Furthermore, cancer-related circRNA-miRNA axis analyses revealed that hsa_circRNA_100375 and its four connected MREs contributed to a cancer-related pathway. The expressions of hsa_circRNA_100375 and hsa_circRNA_401955 were increased significantly in the tumor tissues according to q-PCR.

Conclusion: CircRNA dysregulation was involved in the tumorigenesis of EC. The key circRNAs of hsa_circRNA_401955 and hsa_circRNA_100375 may serve as potential biomarkers and therapeutic targets for EC.

Background

Esophageal carcinoma (EC) ranks as the eighth cause of morbidity and the sixth cause of mortality worldwide, and China has the highest incidence globally [1]. Currently, the overall 5-year survival rate of EC patients remains very low as these patients are always diagnosed at an advanced stage [2, 3]. Therefore, it is crucial to identify new biomarkers and therapeutic targets to improve the diagnosis and treatment of EC.

Noncoding RNAs (ncRNAs) are encoded by approximately 98% of the genome and play important roles in gene expression and regulation [4]. Noncoding circular RNAs (circRNAs) comprise a particular group of endogenous RNAs that are generated from exons transcripts through a back-splicing mechanism, and include exonic, intronic and retained-intron circRNAs [5–7]. CircRNAs have no 5' to 3' polarity or polyA tails; thus, they are expressed stably and widely in mammalian cells, which raises the possibility that circRNAs may serve as biomarkers for use in disease diagnosis. Recent studies have shown that circRNAs can provide a novel type of biomarker for cancer [8, 9], hepatic steatosis [10], and chronic thromboembolic pulmonary hypertension [11]. Reportedly, circRNAs play a crucial role in the development of certain diseases, such as atherosclerotic vascular disease, Alzheimer's disease and cancer [12–14]. Several studies have found that circRNAs may be function as a microRNA (miRNA) sponge and may compete with endogenous RNA networks [15–17]. However, little is known about whether circRNAs can be used as biomarkers for the diagnosis and medical treatment of EC.

Although promising findings have been reported regarding circRNAs in some cancers, no studies have focused on profiling circRNA expression in EC. Thus, we profiled circRNA expression in EC patients and performed bioinformatic analyses, thereby identifying potential circRNAs that may represent biomarkers and candidate therapeutic targets for use in treating EC.

Methods

Samples collection for microarray analysis

All tumor samples were obtained from the Panyu Central Hospital and the Third Affiliated Hospital of Southern Medical University between February 7 and May 2, 2017. All patients were male with an average age of 63.40 ± 2.97 years, and were diagnosed through clinical pathology (three patients had moderately differentiated squamous esophageal carcinomas; one

patient had a highly differentiated squamous esophageal carcinoma; and one had a moderately differentiated tubular adenocarcinoma of the esophagus). All samples were stored at -80°C after collection. The ten samples, including the five tumors and five normal adjacent tissues, which served as controls, were sent to KANGCHEN (Shanghai, China) for Arraystar circRNA microarray analysis.

RNA isolation

Total RNA was extracted from the samples using TRIzol reagent (Invitrogen Corp., USA) according to the manufacturer's instructions. After purification, RNA concentration and quality were determined using a NanoDrop ND-1000 spectrophotometer (NanoDrop, DE, USA). The OD260/OD280 and OD260/OD230 ratios were measured, and the RNA quality considered suitable for research. RNA integrity was confirmed using a denaturing agarose gel electrophoresis.

Validation of RNA sample quality

Total RNA was extracted from all samples, and the RNA quality was assessed by spectrophotometry. The OD260/OD280 ratios of the ten samples were between 1.77 and 1.98, whereas the OD260/OD230 ratios were between 1.99 and 2.38, indicating suitable RNA quality.

Sample labeling, microarray hybridization and analysis

The Arraystar human circRNA microarray (Arraystar, Rockville, USA) was used to detect and analyze the ten samples. Briefly, total RNAs were digested with RNase R (Epicentre, Inc.) to exclude linear RNAs and enrich circRNAs. The enriched circRNAs were then amplified and transcribed with fluorescent cRNA using a random priming method (Arraystar Super RNA Labeling Kit; Arraystar). CRNAs with the label were purified using the RNeasy Mini Kit (Qiagen, Germany). After the labeled cRNAs were fragmented, blocking agent and the fragmentation buffer mixture were heated to 60°C for 30 min, and hybridization buffer was added to dilute the labeled cRNAs. Then, the hybridization solution was dispensed onto a gasket slide, which was assembled with the circRNA expression microarray slide. The slides were incubated for 17 hours at 65°C in an Agilent hybridization oven. Finally, the hybridized arrays were washed, fixed and scanned using an Agilent G2505C Scanner. Differentially expressed (DE) circRNAs were identified using the Arraystar platform. The circRNAs were selected as significantly expressed genes with fold change (FC) values ≥ 1.5 and p-values < 0.05 . Their cluster pattern, scatterplot and volcano plot were analyzed [18, 19].

Prediction of circRNA-miRNA interactions and construction of the circRNA-miRNA coexpression network

CircRNA has been shown to act as an endogenous miRNA sponge and inhibits miRNA-mediated gene expression through miRNA sequestration. To further analyze our results, the circRNA-miRNA interaction was predicted using Arraystar's in-house software (miRNA target prediction) based on TargetScan and miRanda [20, 21]. To identify potential associations between the circRNA and miRNA, we selected 50 significantly DE circRNAs (including 35 upregulated and 15 downregulated circRNAs); these 50 circRNAs were screened using a threshold of FC ≥ 2.0 and p-value < 0.05 , to construct a coexpression network using Cytoscape 3.4.0. The resulting nodes represent the five putative miRNAs that were the most connected functionally to each circRNA.

Spearman correlation test of DE circRNAs in EC patients

To further elucidate whether there was a relevant effect between the 50 DE circRNAs, the Spearman correlation test was performed on the expression levels using Excel2007. Then, the circRNAs were screened according to the criteria: $0.95 \leq \text{Pearson correlation coefficient (PCC)} < 1$ and $-1 < \text{PCC} < -0.95$. The most-related circRNA was selected as the hub gene to construct the coexpression network using Cytoscape. Finally, the hub circRNA and its five connected MREs were subjected to further bioinformatic analysis of circRNA-miRNA interactions, miRNA-mRNA interactions, miRNA target gene prediction and KEGG analysis. KEGG analysis was performed using TarBase included in the software of ClueGO from Cytoscape.

Prediction of cancer-related circRNA-miRNA and KEGG pathway

To determine whether the significant DE of 50 circRNAs was related to EC tumorigenesis, we used the DIANA-MiRpath v.3 platform to predict cancer pathway miRNAs and cancer-related miRNAs using a KEGG reverse search, in TarBase 7.0, based on a p-value threshold of 0.05 [22]. The predicted miRNAs were identified from the initial list of 221 MREs obtained from the Arraystar analysis. After the cancer-related circRNA-miRNA axis was identified, the target genes of the miRNAs were predicted using the miTarBase software option included in CluePedia of Cytoscape. Finally, the KEGG pathway of circRNA-miRNA-mRNAs was predicted using ClueGO in Cytoscape. The axis predicting a cancer-related pathway was further analyzed for its protein association using the string software option in ClueGO. A p-value of ≤ 0.05 was set as the threshold.

PCR sample collection

All tissue samples were collected from the Panyu Central Hospital and the Third Affiliated Hospital of Southern Medical University between October 6, 2014, and May 2, 2017. All patients were male with an average age of 63.20 ± 6.20 years, and were diagnosed through pathology (Fourteen patients had squamous esophageal carcinomas, one patient had adenocarcinoma). The samples were stored at -80°C after collection. The thirty samples, comprising the fifteen tumors and fifteen normal adjacent tissues used as controls, were analyzed for the gene expressions of hsa_circRNA_401955, and hsa_circRNA_100375, and the top three upregulated and the top five downregulated circRNAs were identified using real-time PCR.

Real-time PCR detection

Total RNA was extracted from all samples according to the processing instructions. First-strand cDNA was synthesized using 1 μg of total RNA per sample (Gene copoeia, Inc, USA). Subsequently, the cDNA samples were amplified (Gene copoeia, Inc, USA) in a final volume of 20 μl in an ABI Vii7 dx instrument (ABI, USA). Amplifications were performed as follows: 2 min at 50°C , followed by denaturation for 30 s at 95°C , and 45 cycles of 95°C for 5 s, and 60°C for 34 s. The experiments were carried out in triplicate. β -actin was used as an endogenous reference control. The relative gene expression level was calculated using the $2^{-\Delta\Delta\text{Ct}}$ method. The primer pairs for circRNAs and β -actin are shown in Table 1.

Data analysis

Agilent Feature Extraction software (version 11.0.1.1) was used to analyze the acquired array images. The R software package limma was used for data quantile normalization and analysis. The significance of the differences between the tumor and normal adjacent tissue was estimated using t-test. CircRNAs with $\text{FC} \geq 1.5$ and p-values < 0.05 were selected as significantly DE circRNAs for the cluster, scatter and volcano plot analyses. A p-value < 0.05 was considered significant. A Spearman correlation test was performed using the correlation coefficient method of data analysis in Excel2007.

Data access

Microarray data for all the samples have been deposited in the Gene Expression Omnibus (GEO) under the accession number of GSE103104.

Results

Validation of the RNA sample quality

RNA sample quality was assessed by electrophoresis. RNA integrity was shown to be suitable, and no evidence of DNA contamination was observed (*Fig. 1a*).

CircRNA expression profiling of EC patients

The Arraystar Human circRNA Microarray was used to identify DE circRNAs in the EC tumors and the normal adjacent tissues. A total of 11926 circRNAs were detected by the microarray. After normalization of the raw data, 102 circRNAs were identified as being significantly upregulated and 67 as being downregulated in the tumor tissues by screening for \log_2 FC values greater

than 1.5 and P values ≤ 0.05 . However, only 35 circRNAs were identified as being significantly upregulated, and 15 were identified as being downregulated by screening for FC values greater than 2.0 and P values ≤ 0.05 (Table 2).

Ha_circRNA_043621 and hsa_circRNA_102459 were identified as having the most significant upregulated and downregulated fold changes, respectively. Hierarchical clustering analysis at the expression levels of the circRNAs was performed for the samples (Fig. 2). Scatterplot and volcano plot visualization were constructed to distinguish differences in expression of the circRNAs in the tumor and normal adjacent tissues (Fig. 1b).

Prediction of the miRNA response elements (MREs) of circRNAs and construction of the circRNA-miRNA coexpression network

CircRNA-miRNA interactions were predicted using the Arraystar in-house software (miRNA target prediction). A total of 221 MREs were predicted to combine with the DE circRNAs based on our predefined FC >2.0 and p-value <0.05 thresholds (Table 2). A circRNA-miRNA coexpression network was constructed to show the potential associations among the circRNAs and miRNAs (Fig. 3).

Spearman correlation test of DE circRNAs

The PCC value was analyzed using Spearman's correlation test. Values between 0.95 and 1 and between -1 and -0.95 were chosen to calculate the association between the two circRNAs. The result showed that hsa_circRNA_401955 had six PCC values (0.970 with hsa_circRNA_406487, 0.976 with hsa_circRNA_092512, 0.981 with hsa_circRNA_400082, 0.958 with hsa_circRNA_404864, 0.973 with hsa_circRNA_074306, and 0.990 with hsa_circRNA_055755) within the above ranges and was thus considered the most-connected circRNA. The relation network of the hub circRNA and its connected circRNAs is shown in Fig. 4. Red and green nodes represent upregulated and downregulated circRNAs, respectively. From the circRNA-miRNA coexpression network, we identified that hsa_circRNA_401955 was connected to hsa-miR-141-5p, hsa-miR-642a-5p, hsa-miR-1277-5p, hsa-miR-3064-5p and hsa-miR-6504-5p. The combined sites between the circRNA and the MREs were predicted by Arraystar in-house software (miRNA target prediction) (Fig 5a). KEGG pathway analysis showed that four primary pathways (including mRNA surveillance, cytoskeleton actin regulation, the spliceosome and NOD-like receptor signaling pathway) in the target gene of MREs, were associated with the hub circRNA (Fig. 6) ($P \leq 0.05$).

Prediction of cancer-related circRNA-miRNA target genes and KEGG pathways to further understand the molecular mechanisms of the circRNAs, cancer pathway and cancer-related miRNAs were predicted using DIANA-MiRpath v.3 and identified from the initial list of 221 MREs. Four miRNA axes were identified among the MREs (1. hsa-miR-324-3p/hsa-miR-29a-5p/hsa-miR-485-3p/hsa-miR-149-5p; 2. hsa-miR-485-5p/hsa-miR-574-5p/hsa-miR-454-3p/ hsa-let-7g-3p; 3. hsa-miR-26b-3p/hsa-miR-382-5p /hsa-miR-181a-3p/hsa-miR-330-5p and 4. hsa-miR-138-5p/ hsa-miR-338-3p/ hsa-miR-135b-5p/hsa-miR-135a-5p). From the circRNA-miRNA coexpression network, we identified that these MREs were interacting with hsa_circRNA_100375, hsa_circRNA_400082, hsa_circRNA_102034 and hsa_circRNA_101319. The target genes of the interacting miRNAs axis were predicted using the miRTarBase software option included in CluePedia of Cytoscape. The KEGG pathway of the miRNA-mRNA network was constructed using ClueGo. The result showed that the axis of hsa_circRNA_100375-hsa-miR-324-3p/hsa-miR-29a-5p/hsa-miR-485-3p/hsa-miR-149-5p was involved a cancer-related pathway (Fig. 7a). The seed sequence of the combined sites of the circRNA and four miRNAs was obtained using the Arraystar in-house software (miRNA target prediction) (Fig. 5b). Finally, we further analyzed the proteins in a cancer-related pathway with their two closely related neighborhoods. The results showed that fibroblast growth factor receptor 1 (FGFR1), prostaglandin E receptor 2 (PTGER2), Wnt family member 9B (WNT9B), Wnt family member 2B (WNT2B), Sp1 transcription factor (SP1), CREB binding protein (CREBBP), interleukin 6 (IL-6) and disheveled segment polarity protein2 (DVL2) played key roles in the pathway (Fig. 7b).

Real-time PCR validation

The results showed that the expressions of hub genes hsa_circRNA_401955 and hsa_circRNA_100375 were significantly increased in the tumor samples compared to the normal adjacent tissues in the patients with esophageal carcinoma (p-value <0.05, Fig. 8a). The three top upregulated circRNAs (hsa_circRNA_043621, hsa_circRNA_087961, and hsa_circRNA_404474)

and the five top downregulated circRNAs (hsa_circRNA_102034, hsa_circRNA_100191, hsa_circRNA_101009, hsa_circRNA_102459 and hsa_circRNA_037767) identified were also validated by q-PCR. The results showed that the relative gene expressions of the upregulated circRNAs were all significantly increased while the downregulated circRNAs were decreased in the tumor samples compared to the controls (p -value <0.05 , *Fig. 8b*).

Discussion

In recent years, circRNA has become an important research topic because its key role in gene expression regulation was identified [23]. Following their discovery in RNA viruses, circRNAs were initially regarded as splicing errors [24]. With the development of sequencing technology, more than seven thousand human diseases related to circRNAs have been found [25] and have been reported to promote progression in certain cancers or the development of diseases such as atherosclerosis and nervous system diseases [15, 16, 26–29]. Three types of circRNAs exist: exonic circRNA (the 5' end connects to the 3' end as a cyclic annular form), circular intronic RNA (the 5' end connects to the 2' end as a cyclic annular form), and exon-intron circular RNAs (induced by reverse splicing, these RNAs connect with exons and introns) [30, 31]. CircRNAs are widely expressed and demonstrated with stability, conservation and tissue specificity, properties that are perfectly suited for biomarkers that can be used in disease diagnosis [32].

In this study, we found 169 significantly DE circRNAs, including 102 upregulated and 67 downregulated circRNAs, in EC tumors compared to normal adjacent tissues based on a microarray analysis. The three top upregulated circRNAs and the five top downregulated circRNAs identified were validated by q-PCR. The results showed that the relative gene expressions of the upregulated circRNAs were significantly increased while gene expression of the downregulated circRNAs were decreased in the tumor samples compared to the normal adjacent tissues of EC patients. These findings indicate that circRNA dysregulation may be associated with EC tumorigenesis and that certain key circRNAs may represent candidate biomarkers for EC.

It has been reported that certain circRNAs, especially exonic circRNAs, can inhibit the miRNA-mediated regulation of gene expression by sequestering the relevant miRNAs [33]. These circRNAs combine with miRNAs and inhibit the degradation of mRNAs through competitive integration with miRNAs [34]. CircRNAs function as miRNA sponges (for example, ciRS-7, which adsorbs to miRNA-7 through its binding site and hence quenches normal miRNA-7 functions) [35–37]. These findings indicate that circRNA can directly suppress miRNAs thus inhibiting downstream miRNA target genes, thereby acting as a feedback loop in the circRNA-miRNA-mRNA network.

In our study, we identified circRNA-miRNA interactions using Arraystar in-house software (miRNA target prediction). In total, 221 MREs were predicted to combine with the DE circRNAs based on our predefined $FC > 2.0$ and p -value < 0.05 thresholds. The Spearman correlation test result showed that hsa_circRNA_401955 was the most connected circRNA and was therefore regarded as the hub. This circRNA is an exonic circRNA and is located on chr18 from 32386182 to 32392077, which is annotated as hsa_circ_0108310 in circBase and its gene symbol is **dystrobrevin alpha** (DTNA). This gene reported encodes a cytoskeleton-interacting membrane protein, involved in the formation and stability of synapses in the permeability of the blood-brain barrier and may be related to congenital heart malformation [38–39]. However, the role of hsa_circRNA_401955 has not been studied in cancer. Based on the MRE analysis, we observed that five MREs (hsa-miR-141-5p, hsa-miR-642a-5p, hsa-miR-1277-5p, hsa-miR-3064-5p and hsa-miR-6504-5p) were connected to this hub circRNA. Recent studies have shown that hsa-miR-141-5p is significantly upregulated in ovarian cancer tissue compared to normal tissue [40]. Hsa-miR-642a-5p was identified as the competing endogenous RNA in regulating Linc00974 and KRT19 to affect the proliferation and invasion of hepatocellular carcinoma [41]. Hsa-miR-1277-5p was determined to be a prognostic marker for colorectal cancer staging [42]. Hsa-miR-3064-5p was found to be down-regulated in aristolochic acid (AAN) upper urinary tract carcinoma (UUC) and in non-AANUUC based on miRNA microarray profiling analysis [43]. Hsa-miR-6504-5p was found to target TRAF3 interacting protein 2 (TRAF3IP2), which plays a central role in the innate immune system response to pathogens, inflammatory signals and stress [44]. KEGG analysis showed that four primary pathways (mRNA surveillance, cytoskeleton actin regulation, the spliceosome and the NOD-like receptor signaling pathway) were predicted within the hub circRNA-miRNA-mRNA network.

These results indicate that the hub circRNA and the genes in the pathway represent the potential therapeutic targets and may help to advance our understanding of the mechanism underlying EC tumorigenesis.

To further analyze the role of the circRNA-miRNA in EC patients, we used the DIANA-MiRpath v.3 platform to predict the cancer-related miRNAs. Interestingly, four miRNA axes were identified from the MREs. From the circRNA-miRNA coexpression network, we observed that the four axes were combined with the four circRNAs (hsa_circRNA_100375, hsa_circRNA_400082, hsa_circRNA_102034 and hsa_circRNA_101319, respectively). MiRNAs always negatively regulate their target genes [45–47]. To identify the key pathway in the four miRNA axes, we used the miRTarBase software implemented in CluePedia of Cytoscape to predict the miRNA target genes [48] and used ClueGo to predict the KEGG pathway. The results showed that hsa_circRNA_100375/hsa-miR-324-3p/hsa-miR-29a-5p/hsa-miR-485-3p/hsa-miR-149-5p axis was involved in a cancer-related pathway. Hsa_circRNA_100375 is also exonic and is located on chr1 from 165859440 to 165860559, which is annotated as hsa_circ_0006758 in circBase and its gene symbol is uridine-cytidine kinase 2 (UCK2). UCK2 has been reported to encode a pyrimidine ribonucleoside kinase (the functions of which include the phosphorylation of uridine and cytidine to uridine monophosphate (UMP) and cytidine monophosphate (CMP), respectively) and has been implicated in the uncontrolled proliferation of abnormal cells, a hallmark of cancer [49]. It has been reported that hsa-miR-324-3p was related to kidney cancer [50]. Hsa-miR-29a-5p is significantly downregulated in laryngeal carcinoma [51]. Hsa-miR-485-3p was found to be significantly downregulated in stage II colorectal cancer (CRC) tumors compared to normal tissues [52]. Hsa-miR-149-5p contains a binding site for the long noncoding RNA MALAT1, which promotes the development of triple-negative breast cancer [53]. KEGG pathway analysis of in the cancer-related axis showed that certain hub proteins, such as FGFR1, PTGER2, WNT9B, WNT2B, SP1, CREBBP, IL-6 and DVL2, may play a key role in this pathway. These hub proteins and hsa_circRNA_100375 may be regarded as the key genes regulating EC tumorigenesis.

Finally, the expression of hsa_circRNA_100375 and hsa_circRNA_401955 was detected in fifteen EC patients by PCR. The results showed that these two hub circRNAs were significantly increased in the tumor samples compared to the normal adjacent tissues. These results indicate that the two circRNAs play a key role in EC.

Conclusion

In conclusion, circRNA dysregulation is involved in EC tumorigenesis. Hsa_circRNA_401955 was found to be the hub circRNA, and four primary pathways were predicted to occur in this hub circRNA-miRNA-mRNA network. Hsa_circRNA_100375 and its associated of MRE axis are involved in a cancer-related pathway. Several key circRNAs and proteins may serve as potential biomarkers and therapeutic targets for EC. Furthermore, our findings may improve our understanding of the EC tumorigenesis mechanism. However, this study is limited by the relatively small sample size. Our results showed some effects of circRNAs in EC tumorigenesis. Nevertheless, the precise mechanism remains to be elucidated.

Declarations

Funding

This work was supported by the grants from the Technical NewStar of Zhujiang, Pan Yu District, Guangzhou (2013-special-15-6.10) and the Science and Technology Program of Guangzhou (201804010012 and 201904010065).

Availability of data and materials

The datasets used and/or analysed during this study are available from the corresponding author on reasonable request.

Authors' contributions

XhC and SnC performed the analysis of the data and writing of the paper. Xn Z, Lp W and Hl L collected the samples. SnC and Wh L performed the experiments.

Competing interests

The authors declare no conflict of interest.

Consent for publication

Not applicable

>Ethics approval and consent to participate

The study was approved by the Ethics Committee of the Panyu Central Hospital. All patients agreed to participate and gave their informed consent in this study.

References

1. Siegel RL, Miller KD, Jemal A. Cancer Statistics, 2017. *CA Cancer J Clin.* 2017; 67(1): 7–30.
2. Hikami S, Shiozaki A, Fujiwara H, Konishi H, Arita T, Kosuga T, Morimura R, Murayama Y, Komatsu S, Ikoma H, et al. [Outcome of Patients with Pathological Complete Response after Neoadjuvant Chemotherapy in Advanced Esophageal Cancer](#) *Gan To Kagaku Ryoho.* 2017; 44(12):1796–1798.
3. Saddoughi SA, Reinersman JM, Zhukov YO, Taswell J, Mara K, Harmsen SW, Blackmon SH, Cassivi SD, Nichols F, Shen KR, et al. Survival After Surgical Resection of Stage IV Esophageal Cancer. *Ann Thorac Surg.* 2017; 103 (1): 261–6.
4. Zhang Y, Xue W, Li X, Zhang J, Chen S, Zhang JL, Yang L, Chen LL. The Biogenesis of Nascent Circular RNAs. *Cell Rep.* 2016; 15 (3): 611–24.
5. Liang D, Wilusz JE. Short intronic repeat sequences facilitate circular RNA production. *Genes Dev.* 2014; 28(20): 2233–47.
6. Greene J, Baird AM, Brady L, Lim M, Gray SG. Biogenesis, Function and Role in Human Diseases. *Front Mol Biosci.* 2017; 4: 38.
7. Beermann J, Piccoli MT, Viereck J, et al. Non-coding RNAs in Development and Disease: Background, Mechanisms, and Therapeutic Approaches. *Physiol Rev.* 2016; 96(4): 1297–325.
8. Zhang HD, Jiang LH, Sun DW, Hou JC, Ji ZL. CircRNA: a novel type of biomarker for cancer. *Breast Cancer.* 25(1):1–7.
9. Meng S, Zhou H, Feng Z, Xu Z, Tang Y, Li P, Wu M. CircRNA: functions and properties of a novel potential biomarker for cancer. *Mol Cancer.* 16(1): 94.
10. Guo XY, He CX, Wang YQ, un C, Li GM, Su Q, Pan Q, Fan JG. Circular RNA Profiling and Bioinformatic Modeling Identify Its Regulatory Role in Hepatic Steatosis. *Biomed Res Int.* 2017; 2017: 5936171.
11. Miao R, Wang Y, Wan J, Leng D, Gong J, Li J, Liang Y, Zhai Z, Yang Y. Microarray expression profile of circular RNAs in chronic thromboembolic pulmonary hypertension. *Medicine (Baltimore).* 2017; 96(27): e7354.
12. Ren S, Xin Z, Xu Y, Xu J, Wang G. Construction and analysis of circular RNA molecular regulatory networks in liver cancer. *Cell Cycle.* 2017; 16(22):2204–2211.
13. Rong D, Sun H, Li Z, Liu S, Dong C, Fu K, Tang W, Cao H. An emerging function of circRNA-miRNAs-mRNA axis in human diseases. *Oncotarget.* 2017; 8(42):73271–73281.
14. Huang S, Yang B, Chen BJ, Bliim N, Ueberham U, Arendt T, Janitz M.

The emerging role of circular RNAs in transcriptome regulation. *Genomics*. 2017; 109(5–6):401–407.

15. Liang HF, Zhang XZ, Liu BG, Jia GT, Li WL. Circular RNA circ-ABC10 promotes breast cancer proliferation and progression through sponging miR-1271. *Am J Cancer Res*. 2017; 7(7): 1566–76.
16. Zhong Z, Huang M, Lv M, He Y, Duan C, Zhang L, Chen J. Circular RNA MYLK as a competing endogenous RNA promotes bladder cancer progression through modulating VEGFA/VEGFR2 signaling pathway. *Cancer Lett*. 2017; 403: 305–17.
17. Zhang H, Wang G, Ding C, Liu P, Wang R, Ding W, Tong D, Wu D, Li C, Wei Q, et al. Increased circular RNA UBAP2 acts as a sponge of miR-143 to promote osteosarcoma progression. *Oncotarget*. 2017; 8(37):61687–61697.
18. Liu YC, Li JR, Sun CH, Andrews E, Chao RF, Lin FM, Weng SL, Hsu SD, Huang CC, Cheng C, et al. CircNet: a database of circular RNAs derived from transcriptome sequencing data. *Nucleic Acids Res*. 2016; 44(D1): D209–15.
19. Ghosal S, Das S, Sen R, Basak P, Chakrabarti J. Circ2Traits: a comprehensive database for circular RNA potentially associated with disease and traits. *Front Genet*. 2013; 4: 283.
20. Enright AJ, John B, Gaul U, Tuschl T, Sander C, Marks DS. MicroRNA targets in *Drosophila*. *Genome Biol*. 2003; 5(1): R1.
21. Pasquinelli AE. MicroRNAs and their targets: recognition, regulation and an emerging reciprocal relationship. *Nat Rev Genet*. 2012; 13(4): 271–82.
22. Vlachos IS, Zagganas K, Paraskevopoulou MD, Georgakilas G, Karagkouni D, Vergoulis T, Dalamagas T, Hatzigeorgiou AG. DIANA-miRPath v3.0: deciphering microRNA function with experimental support. *Nucleic Acids Res*. 2015; 43(W1): W460–6.
23. Jeck WR, Sorrentino JA, Wang K, Slevin MK, Burd CE, Liu J, Marzluff WF, Sharpless NE. Circular RNAs are abundant, conserved, and associated with ALU repeats. *Rna*. 2013; 19(2): 141–57.
24. Sanger HL, Klotz G, Riesner D, Gross HJ, Kleinschmidt AK. Viroids are single-stranded covalently closed circular RNA molecules existing as highly base-paired rod-like structures. *Proc Natl Acad Sci U S A*. 1976; 73(11): 3852–6.
25. Memczak S, Jens M, Elefsinioti A, Torti F, Krueger J, Rybak A, Maier L, Mackowiak SD, Gregersen LH, Munschauer M, et al. Circular RNAs are a large class of animal RNAs with regulatory potency. *Nature*. 2013; 495(7441): 333–8.
26. Huang YS, Jie N, Zou KJ, Weng Y. Expression profile of circular RNAs in human: astric cancer tissues. *MolMed Rep*. 2017; 16(3): 2469–76.
27. Huang G, Li S, Yang N, Zou Y, Zheng D, Xiao T. Recent progress in circular RNAs in human cancers. *Cancer Lett*. 2017; 404: 8–18.
28. Kumar L, Shamsuzzama, Haque R, Baghel T, Nazir A. Circular RNAs: the Emerging Class of Non-coding RNAs and Their Potential Role in Human Neurodegenerative Diseases. *Mol Neurobiol*. 2017; 54(9):7224–7234.
29. Burd CE, Jeck WR, Liu Y, Sanoff HK, Wang Z, Sharpless NE. Expression of linear and novel circular forms of an INK4/ARF-associated non-coding RNA correlates with atherosclerosis risk. *PLoS Genet*. 2010; 6(12): e1001233.
30. Zhang XO, Wang HB, Zhang Y, Chen L, Lu X, Chen LL, Yang L. Complementary sequence-mediated exon circularization. *Cell*. 2014; 159(1): 134–47.
31. Li Z, Huang C, Bao C, Chen L, Lin M, Wang X, Zhong G, Yu B, Hu W, Dai L, et al. Exon-intron circular RNAs regulate transcription in the nucleus. *Nat Struct Mol Biol*. 2015; 22(3): 256–64.

32. Schwanhaussner B, Busse D, Li N, Dittmar G, Schuchhardt J, Wolf J, Chen W, Selbach M. Corrigendum. Global quantification of mammalian gene expression control. *Nature*. 2013; 495(7439): 126–7.
33. Hansen TB, Jensen TI, Clausen BH, Bramsen JB, Finsen B, Damgaard CK, Kjems J. Natural RNA circles function as efficient microRNA sponges. *Nature*. 2013; 495(7441): 384–8.
34. Hansen TB, Wiklund ED, Bramsen JB, Villadsen SB, Statham AL, Clark SJ, Kjems J. miRNA-dependent gene silencing involving Ago2-mediated cleavage of a circular antisense RNA. *Embo j*. 2011; 30(21): 4414–22.
35. Peng L, Yuan XQ, Li GC. The emerging landscape of circular RNA ciRS-7 in cancer (Review). *Oncol Rep*. 2015; 33(6): 2669–74.
36. Pan H, Li T, Jiang Y, Pan C, Ding Y, Huang Z, Yu H, Kong D. Overexpression of Circular RNA ciRS-7 Abrogates the Tumor Suppressive Effect of miR-7 on Gastric Cancer via PTEN/PI3K/AKT Signaling Pathway. *J Cell Biochem*. 2018; 119(1):440–446.
37. Zhao Y, Alexandrov PN, Jaber V, Lukiw WJ. Deficiency in the Ubiquitin Conjugating Enzyme UBE2A in Alzheimer's Disease (AD) is Linked to Deficits in a Natural Circular miRNA-7 Sponge (circRNA; ciRS-7). *Genes (Basel)*. 2016; 7(12):pii: E116.
1. Teresa Requena, Sonia Cabrera, Carmen Martín-Sierra, Steven D, Price Anna Lysakowski, José A. Lopez-Escamez. Identification of two novel mutations in FAM136A and DTNA genes in autosomal-dominant familial Meniere's disease, *Hum Mol Genet*. 2015; 24(4):1119–26.
 2. Zlotina A, Nikulina T, Yany N, Moiseeva O, Pervunina T, Grekhov E, Kostareva A. Ring chromosome 18 in combination with 18q12.1 (DTNA) interstitial microdeletion in a patient with multiple congenital defects. *Mol Cytogenet*. 2016; 9:18.
 3. Wang L, Zhu MJ, Ren AM, Wu HF, Han WM, Tan RY, Tu RQ. A ten-microRNA signature identified from a genome-wide microRNA expression profiling in human epithelial ovarian cancer. *PLoS One*. 2014; 9(5):e96472.
 4. Tang J, Zhuo H, Zhang X, Jiang R, Ji J, Deng L, Qian X, Zhang F, Sun B. A novel biomarker Linc00974 interacting with KRT19 promotes proliferation and metastasis in hepatocellular carcinoma. *Cell Death Dis*. 2014; 5:e1549.
 5. Habib Motieghader, Morteza Kouhsar, Balal Sadeghi, Ali Masoudi-Nejad. mRNA-miRNA bipartite network reconstruction to predict prognostic module biomarkers in colorectal cancer stage differentiation. *Mol Biosyst*. 2017; 13(10):2168–2180.
 6. Le Tao, Yigang Zeng, Jun Wang, Zhihong Liu, Bing Shen, Jifu Ge, Yong Liu, Yifeng Guo, Jiangxin Qiu. Differential microRNA expression in aristolochic acid-induced upper urothelial tract cancers ex vivo. *Mol Med Rep*. 2015; 12(5): 6533–6546.
44. Anandaram H. A computational approach to identify microRNA (miRNA) based biomarker from the regulation of disease pathology. *Biol Med Case Rep*. 2018; 2: 12–25.
45. Fujiwara T, Yada T. miRNA-target prediction based on transcriptional regulation. *BMC Genomics*. 2013; 14 Suppl 2: S3.
46. Liu B, Li J, Cairns MJ. Identifying miRNAs, targets and functions. *Brief Bioinform*. 2014; 15(1):1–19.
47. Guo L, Zhao Y, Yang S, Zhang H, Chen F. Integrative analysis of miRNA-mRNA and miRNA-miRNA interactions. *Biomed Res Int*. 2014; 2014: 907420.
48. Bindea G, Galon J, Mlecnik B. CluePedia Cytoscape plugin: pathway insights using integrated experimental and in silico data. *Bioinformatics*. 2013; 29(5): 661–3.
49. Ibrahim Malami, Ahmad Bustamam Abdul, Rasedee Abdullah, Nur Kartinee Bt Kassim, Peter Waziri, Imaobong Christopher Etti. Imaobong Christopher Etti. In silico discovery of potential Uridine-Cytidine Kinase 2 inhibitors from the Rhizome of *Alpinia mutica*. *Molecules* 2016; 21(4):417

50. Petillo D, Kort EJ, Anema J, Furge KA, Yang XJ, Teh BT. MicroRNA profiling of human kidney cancer subtypes. *Int J Oncol.* 2009; 35(1):109–14.

1. Zhong-Ming Lu, Ye-Feng Lin, Li Jiang, Liang-Si Chen, Xiao-Ning Luo, Xin-Han Song, Shao-Hua Chen, Si-Yi Zhang. Micro-ribonucleic acid expression profiling and bioinformatic target gene analyses in laryngeal carcinoma. *Onco Targets Ther.* 2014; 7: 525–533.
2. Chang KH, Miller N, Kheirleiseid EA, Lemetre C, Ball GR; Smith MJ, Regan M, McAnena OJ, Kerin MJ. MicroRNA signature analysis in colorectal cancer: identification of expression profiles in stage II tumors associated with aggressive disease. *Int J Colorectal Dis.* 2011; 26(11):1415–22.

53 Jin C, Yan B, Lu Q, Ma L. Reciprocal regulation of Hsa-miR-1 and long noncoding RNA MALAT1 promotes triple-negative breast cancer development. *Tumour Biol.* 2016, 37(6):7383–94

Tables

Table 1 Primer for circRNAs and β -actin. The primers used for the circRNAs and β -actin in the q-PCR detection.

Gene	primer(5'- 3')
hsa_circRNA_401955	F: AAATTTTCAGTATTTGCTGTCAAAAACA R:CTTCCCTGTTGGGAGAAACA
hsa_circRNA_100375	F: TGTCTCCCATTCCTCGTCTTC R: TAGTCCACCTCATTCTGCCC
hsa_circRNA_102034	F: CAGACAAAGACAGCAGGTTCC R: TGTTGGAAGTCTCTCTGGGG
hsa_circRNA_100191	F: AGGAGGATGAGATGCCAGTT R: CTGGGAGGGATGGAGAAACG
hsa_circRNA_101009	F: TACTTCTCCAGCAACCCCTG R: GGAGAGCAACTACAGTATCCTCA
hsa_circRNA_102459	F: AGACGATCTCTCTGAGGCCTA R: CAGCAGGTGGTAGAACTCCT
hsa_circRNA_037767	F: TCAGCATCCCCAGTTACGAG R: CGATGGCCTTGACCTCATTG
hsa_circRNA_043621	F: GCTGACCTGGAGATGCAGAT R: TGTCTCATACTTGGTGC GGA
hsa_circRNA_087961	F: GGGCGTGATCATGAAAGGTG R: CCGCAGACCTCCTCATTCTA
hsa_circRNA_404474	F: TTCCCGACCTCCAAGTACAC R: TCCTCTAGCATGGCCTTCTG
β -actin	F: ACTCTTCCAGCCTTCCTTCC R: GTACTTGCCTCAGGAGGAG

Table 2 Microarray analysis of circRNAs which were up- or down-regulated in esophageal carcinoma patients. There were 35 up-regulated and 15 down-regulated circRNAs as the fold change more than 2 and p value less than 0.05.

Predicted miRNA response elements(MREs)								
circRNA	P-value	FDR	FC	MRE1	MRE2	MRE3	MRE4	MRE5
upregulation								
hsa_circRNA_028826	0.0361	0.5643	2.0161	hsa-miR-93-3p	hsa-miR-7843-5p	hsa-miR-4530	hsa-miR-4685-5p	hsa-miR-92a-2-5p
hsa_circRNA_053294	0.0091	0.5642	2.0285	hsa-miR-875-3p	hsa-miR-584-5p	hsa-miR-3074-5p	hsa-miR-3622a-3p	hsa-miR-4286
hsa_circRNA_101287	0.0296	0.5643	2.5694	hsa-miR-499a-3p	hsa-miR-526b-5p	hsa-miR-363-3p	hsa-miR-208a-5p	hsa-miR-578
hsa_circRNA_100375	0.0421	0.5668	2.6894	hsa-miR-324-3p	hsa-miR-29a-5p	hsa-miR-580-3p	hsa-miR-485-3p	hsa-miR-149-5p
hsa_circRNA_405813	0.0186	0.5642	2.0341	hsa-miR-665	hsa-miR-6884-5p	hsa-miR-4459	hsa-miR-1285-3p	hsa-miR-1273g-3p
hsa_circRNA_401955	0.0275	0.5643	2.1596	hsa-miR-1277-5p	hsa-miR-3064-5p	hsa-miR-642a-5p	hsa-miR-6504-5p	hsa-miR-141-5p
hsa_circRNA_404905	0.0310	0.5643	2.3807	hsa-miR-8060	hsa-miR-185-5p	hsa-miR-5008-3p	hsa-miR-4793-3p	hsa-miR-656-5p
hsa_circRNA_102339	0.0006	0.5320	2.2427	hsa-miR-875-5p	hsa-miR-215-5p	hsa-miR-192-5p	hsa-let-7a-2-3p	hsa-miR-208a-5p
hsa_circRNA_100045	0.0163	0.5642	2.0009	hsa-miR-764	hsa-miR-149-3p	hsa-miR-650	hsa-miR-659-5p	hsa-miR-93-3p
hsa_circRNA_406487	0.0330	0.5643	2.2969	hsa-miR-297	hsa-miR-541-3p	hsa-miR-155-5p	hsa-miR-153-5p	hsa-miR-4775
hsa_circRNA_092512	0.0396	0.5643	2.0555	hsa-miR-4763-3p	hsa-miR-3619-5p	hsa-miR-7150	hsa-miR-1207-5p	hsa-miR-6756-5p
hsa_circRNA_103923	0.0445	0.5713	2.0984	hsa-miR-429	hsa-miR-23b-5p	hsa-miR-200b-3p	hsa-miR-105-3p	hsa-miR-656-5p
hsa_circRNA_001655	0.0313	0.5643	2.9594	hsa-miR-6813-5p	hsa-miR-5001-5p	hsa-miR-762	hsa-miR-4498	hsa-miR-185-3p
hsa_circRNA_400082	0.0158	0.5642	2.7868	hsa-miR-485-5p	hsa-miR-648	hsa-miR-574-5p	hsa-miR-454-3p	hsa-let-7g-3p
hsa_circRNA_101693	0.0280	0.5643	2.3458	hsa-miR-1301-3p	hsa-miR-384	hsa-miR-141-5p	hsa-miR-646	hsa-miR-373-5p
hsa_circRNA_033628	0.0165	0.5642	3.0872	hsa-miR-4763-3p	hsa-miR-612	hsa-miR-3615	hsa-miR-6511b-5p	hsa-miR-635
hsa_circRNA_043621	0.0089	0.5642	5.3218	hsa-miR-223-3p	hsa-miR-4268	hsa-miR-3692-3p	hsa-miR-657	hsa-miR-6871-3p
hsa_circRNA_405551	0.0382	0.5643	2.3020	hsa-miR-6895-5p	hsa-miR-378i	hsa-miR-1236-3p	hsa-miR-6736-5p	hsa-miR-892b
hsa_circRNA_404474	0.0174	0.5641	3.5533	hsa-miR-6743-3p	hsa-miR-3157-5p	hsa-miR-1205	hsa-miR-378h	hsa-miR-5009-5p
hsa_circRNA_048574	0.0266	0.5643	2.4765	hsa-miR-4725-3p	hsa-miR-6858-5p	hsa-miR-5698	hsa-miR-4723-5p	hsa-miR-7843-5p
hsa_circRNA_084900	0.0051	0.5642	2.3135	hsa-miR-4778-3p	hsa-miR-877-3p	hsa-miR-6881-3p	hsa-miR-5196-3p	hsa-miR-6809-3p
hsa_circRNA_061346	0.0123	0.5642	2.6457	hsa-miR-4778-3p	hsa-miR-5196-3p	hsa-miR-5193	hsa-miR-877-3p	hsa-miR-103a-2-5p
hsa_circRNA_027446	0.0193	0.5642	2.5080	hsa-miR-129-5p	hsa-miR-331-3p	hsa-miR-6882-3p	hsa-miR-3925-3p	hsa-miR-1236-3p
hsa_circRNA_001244	0.0025	0.5598	2.4528	hsa-miR-6861-5p	hsa-miR-619-5p	hsa-miR-1303	hsa-miR-125a-3p	hsa-miR-5787
hsa_circRNA_406748	0.0440	0.5713	3.5072	hsa-miR-5683	hsa-miR-588	hsa-miR-4538	hsa-miR-6740-5p	hsa-miR-7110-3p
hsa_circRNA_067209	0.0400	0.5643	2.3571	hsa-miR-8082	hsa-miR-146b-3p	hsa-miR-6876-3p	hsa-miR-4534	hsa-miR-7112-3p
hsa_circRNA_101877	0.0024	0.5598	2.1485	hsa-miR-449c-5p	hsa-miR-27a-3p	hsa-miR-27b-3p	hsa-miR-887-5p	hsa-miR-636
hsa_circRNA_404864	0.0498	0.5758	2.3992	hsa-miR-4742-3p	hsa-miR-4753-3p	hsa-miR-4516	hsa-miR-7847-3p	hsa-miR-4708-3p
hsa_circRNA_050998	0.0031	0.5642	2.2380	hsa-miR-433-3p	hsa-miR-2277-5p	hsa-miR-937-5p	hsa-miR-1178-5p	hsa-miR-5089-5p
hsa_circRNA_006226	0.0459	0.5713	2.2582	hsa-miR-548a-5p	hsa-miR-548i	hsa-miR-4668-3p	hsa-miR-548ab	hsa-miR-548a-5p
hsa_circRNA_090364	0.0098	0.5642	2.5156	hsa-miR-378h	hsa-miR-378f	hsa-miR-378b	hsa-miR-378c	hsa-miR-378a-3p
hsa_circRNA_089761	0.0318	0.5643	4.0300	hsa-miR-3529-3p	hsa-miR-6891-3p	hsa-miR-554	hsa-miR-5196-3p	hsa-miR-384
hsa_circRNA_071312	0.0340	0.5643	2.2288	hsa-miR-4476	hsa-miR-4722-5p	hsa-miR-377-3p	hsa-miR-1207-5p	hsa-miR-3140-5p
hsa_circRNA_074306	0.0159	0.5642	2.8455	hsa-miR-4763-3p	hsa-miR-3157-5p	hsa-miR-1249-5p	hsa-miR-198	hsa-miR-6797-5p
hsa_circRNA_055755	0.0410	0.5643	2.1324	hsa-miR-7156-3p	hsa-miR-6845-5p	hsa-miR-103a-2-5p	hsa-miR-211-5p	hsa-miR-4685-3p
Downregulation								
hsa_circRNA_102459	0.0219	0.5642	3.8287	hsa-miR-508-5p	hsa-miR-766-3p	hsa-miR-328-3p	hsa-miR-761	hsa-miR-497-3p
hsa_circRNA_102034	0.0168	0.5642	2.9900	hsa-miR-26b-3p	hsa-miR-382-5p	hsa-miR-181a-3p	hsa-miR-330-5p	hsa-miR-125a-3p
hsa_circRNA_060102	0.0338	0.5643	2.1602	hsa-miR-4459	hsa-miR-5787	hsa-miR-6736-5p	hsa-miR-4270	hsa-miR-6804-5p
hsa_circRNA_101009	0.0365	0.5643	2.3586	hsa-miR-653-5p	hsa-miR-509-3p	hsa-miR-584-3p	hsa-miR-370-3p	hsa-miR-93-3p
hsa_circRNA_406963	0.0362	0.5643	2.1734	hsa-miR-4668-5p	hsa-miR-4739	hsa-miR-3153	hsa-miR-608	hsa-miR-372-5p
hsa_circRNA_102033	0.0278	0.5643	2.2037	hsa-miR-382-5p	hsa-miR-330-5p	hsa-miR-26b-3p	hsa-miR-489-3p	hsa-miR-514a-5p
hsa_circRNA_100191	0.0148	0.5642	2.5797	hsa-miR-647	hsa-miR-588	hsa-miR-660-3p	hsa-miR-661	hsa-miR-552-3p
hsa_circRNA_085362	0.0375	0.5643	2.1945	hsa-miR-1248	hsa-miR-1205	hsa-miR-623	hsa-miR-5002-5p	hsa-miR-4753-3p
hsa_circRNA_037767	0.0466	0.5713	2.7396	hsa-miR-1205	hsa-miR-6772-3p	hsa-miR-3907	hsa-miR-1184	hsa-miR-4664-3p
hsa_circRNA_050898	0.0204	0.5642	2.0588	sa-miR-3909	hsa-miR-4691-5p	hsa-miR-1226-5p	hsa-miR-6792-3p	hsa-miR-6762-3p
hsa_circRNA_100239	0.0165	0.5642	2.1057	hsa-miR-602	hsa-miR-22-3p	hsa-miR-320b	hsa-miR-320a	hsa-miR-761
hsa_circRNA_101319	0.0477	0.5729	2.0857	hsa-miR-138-5p	hsa-miR-135a-3p	hsa-miR-338-3p	hsa-miR-135b-5p	hsa-miR-135a-5p
hsa_circRNA_103942	0.0395	0.5643	2.3015	hsa-miR-382-5p	hsa-miR-183-3p	hsa-miR-134-3p	hsa-miR-328-5p	hsa-miR-541-3p
hsa_circRNA_054220	0.0148	0.5642	2.2275	hsa-miR-513b-5p	hsa-miR-4435	hsa-miR-6780b-5p	hsa-miR-335-3p	hsa-miR-4665-5p
hsa_circRNA_402901	0.0015	0.5320	2.0481	hsa-miR-6845-3p	hsa-miR-4279	hsa-miR-450a-2-3p	hsa-miR-520h	hsa-miR-520g-3p

Figures

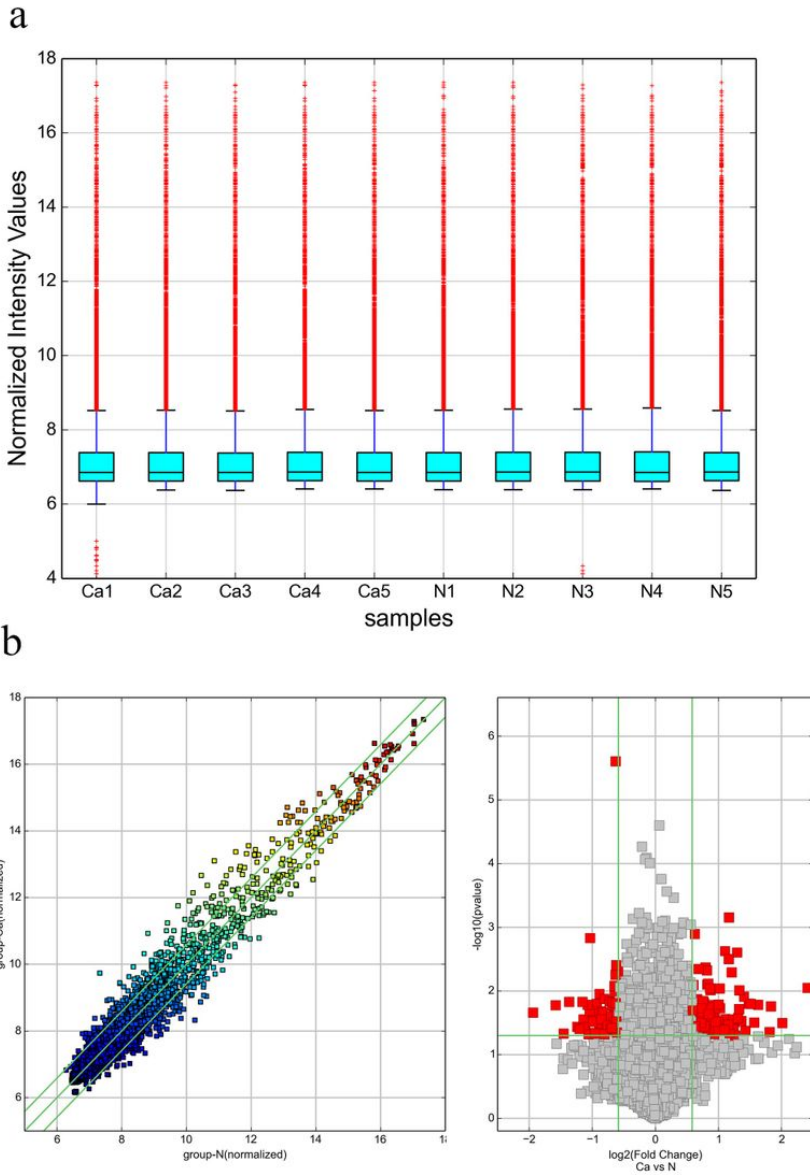


Figure 1

The distribution of circRNAs and distinguishable circRNAs identified through scatter plot and volcano plot. **a**: The distribution of circRNAs show by box plots in the ten samples. After normalization, the distributions were nearly the same. **b1**: Volcano plot of distinguished circRNAs. The dots above the top and the bottom green line revealed that the expression was more than 1.5-fold. **B2**: Volcano plot of circRNAs. The red point represents for 1.5 fold up and down regulated of circRNAs expression.

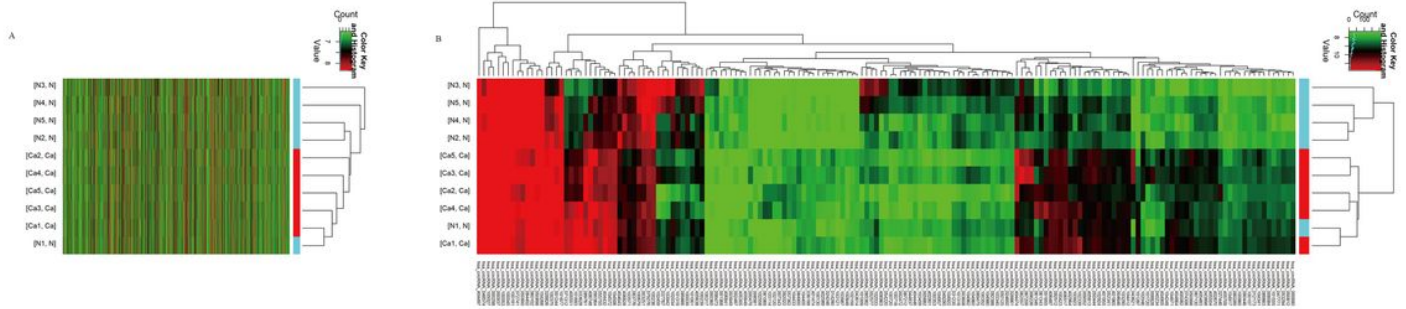


Figure 2

Profiling of circRNAs detected by microarray in esophageal carcinoma patients. a: CircRNA microarray expression data among the ten samples. b: Heat map of the differentially expressed circRNAs. The red represents for the high expression, while the green represents for the low expression.



Figure 3

The coexpression network of circRNA-miRNA. The network of significant differentially expressed circRNAs (fold change more than 2.0) and its connected miRNA response elements (MREs) was constructed by Cytocape. a: the up-regulated circRNA-miRNA coexpression network; b: the down-regulated circRNA-miRNA coexpression network.

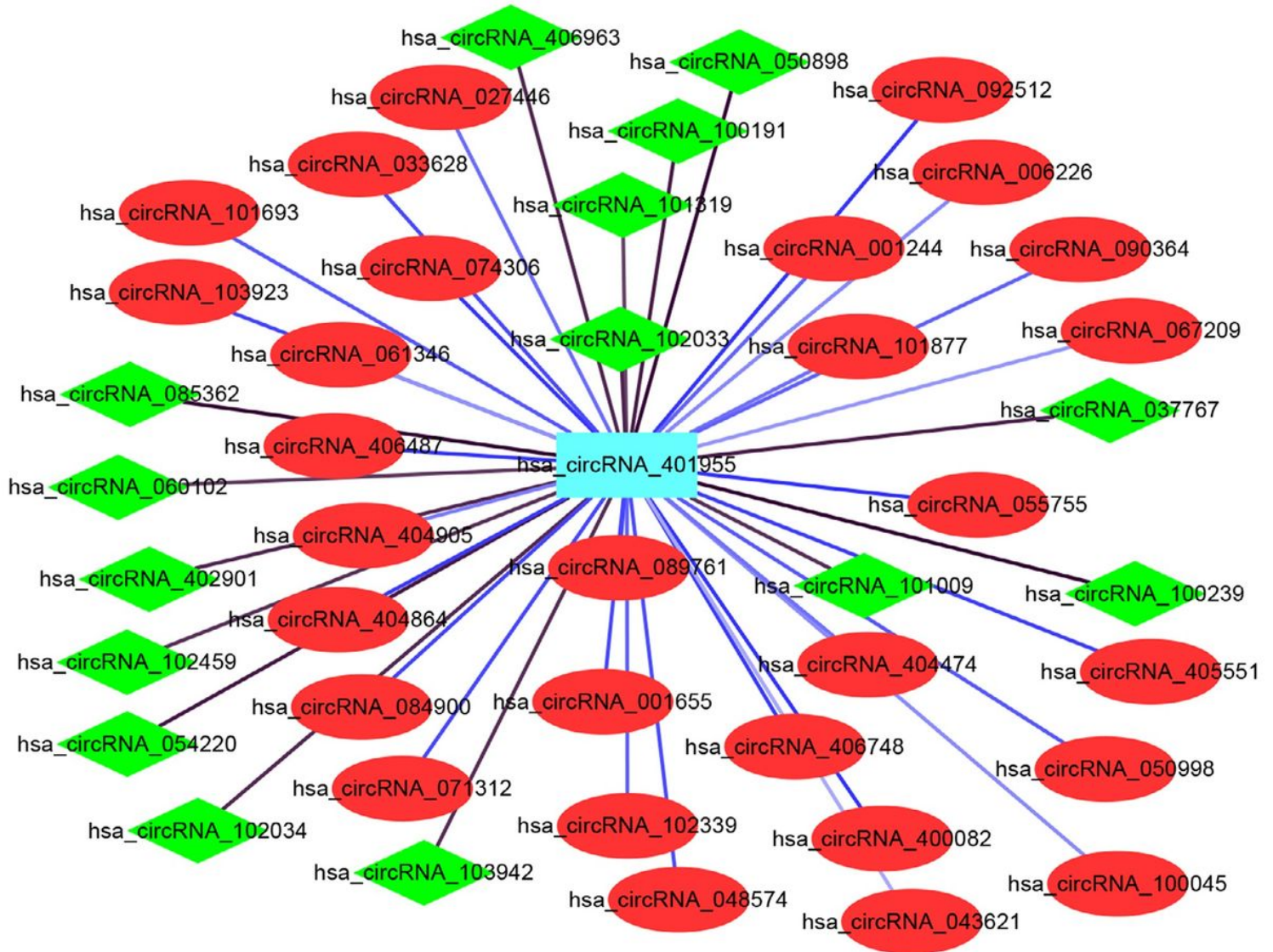
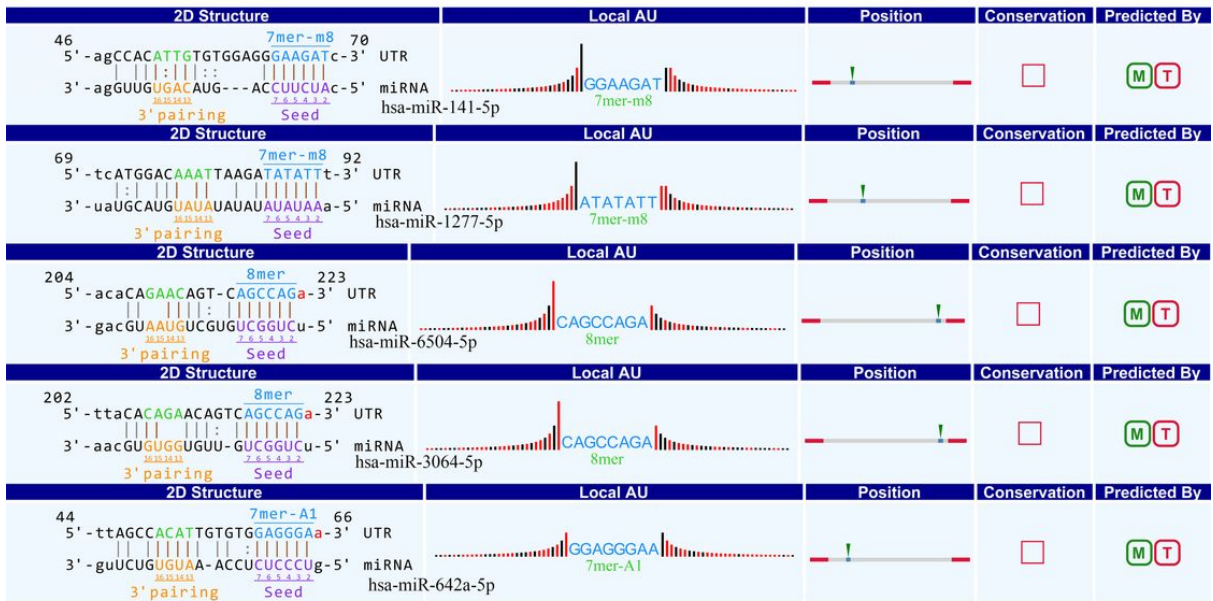


Figure 4

The coexpression network of the hub circRNA and its related circRNAs. The red nodes represent for positive correlation, the green nodes represent for the negative correlation. The colors of the connected lines from black to blue represent for the low to high value of the correlation coefficient.

a



b

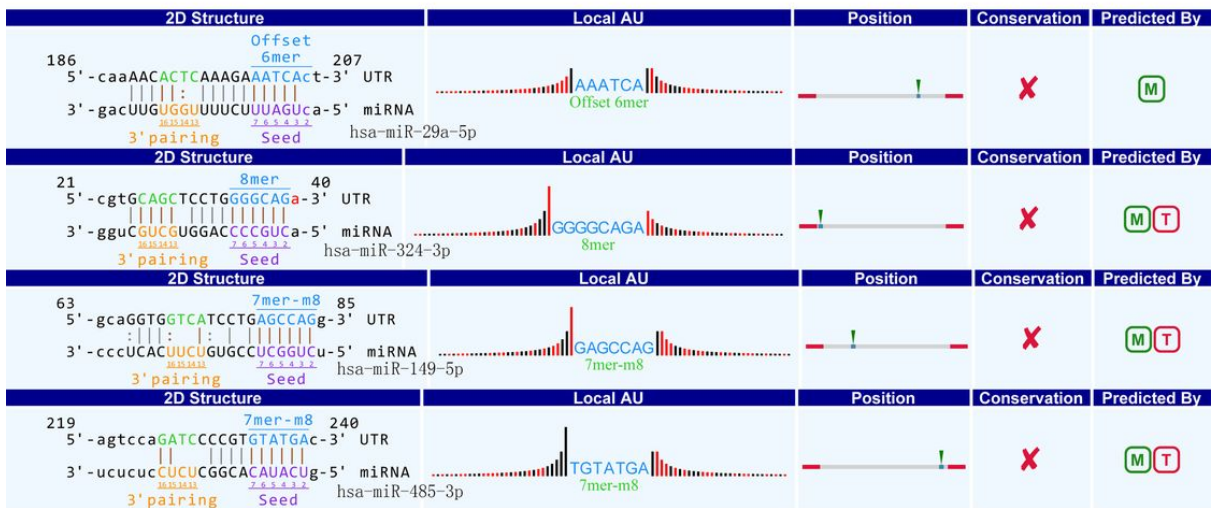


Figure 5

The combined sites of the two hub circRNA (Hsa_circRNA_401955 and hsa_circRNA_100375) and their five connected miRNA response elements (MREs): a: The combined sites of the hub circRNA (Hsa_circRNA_401955) and its five connected miRNA response elements (MREs). b: The combined sites of hsa_circRNA_100375 and its four cancer related miRNA response elements (MREs) (hsa-miR-324-3p / hsa-miR-29a-5p / hsa-miR-485-3p / hsa-miR-149-5p).

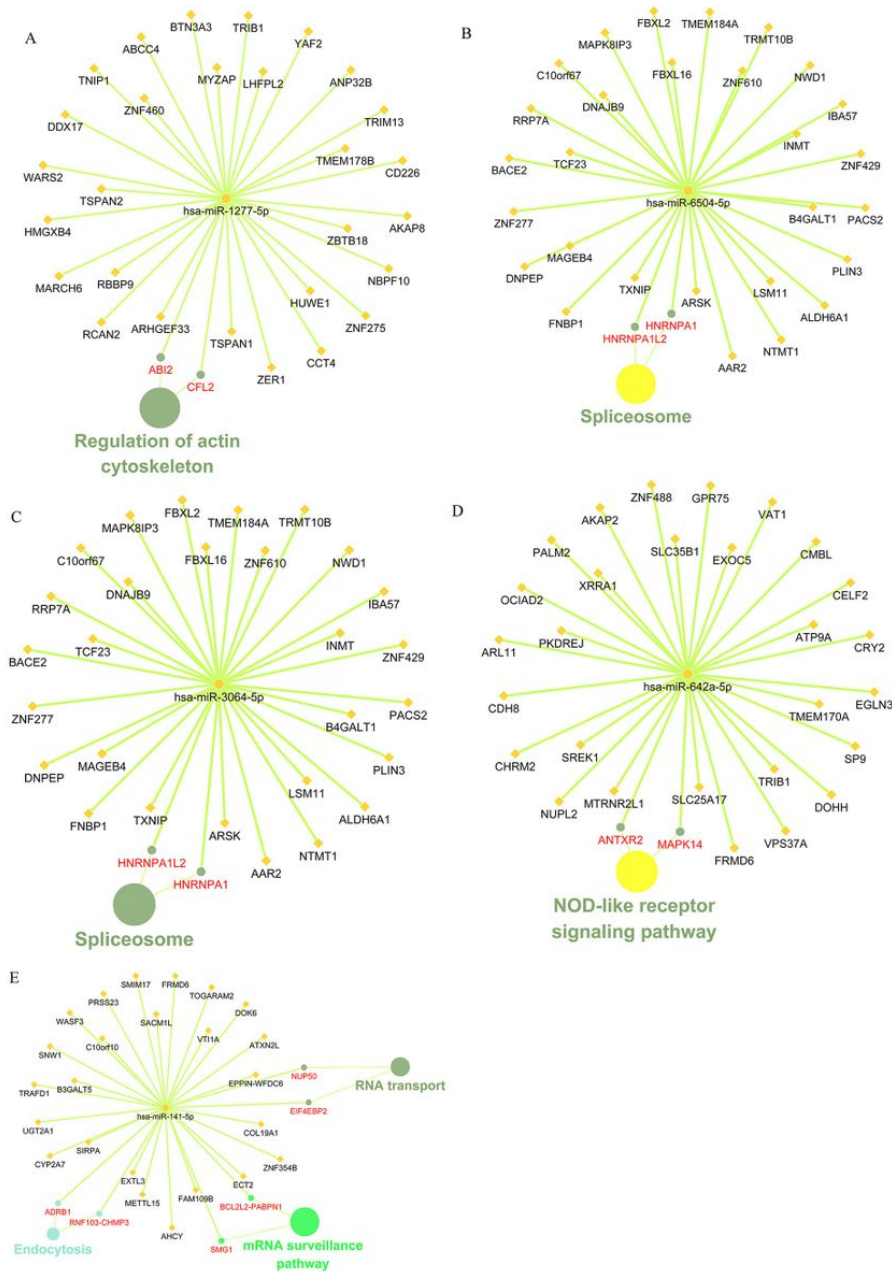


Figure 6

Kyoto Encyclopedia of Genes and Genomes(KEGG) pathway analysis of the hub circRNA's(Hsa_circRNA_401955) related with miRNA response elements (MREs). a, b, c, d, e: KEGG pathway analysis of hsa-miR-1277-5p, hsa-miR-6504-5p, hsa-miR-3064-5p, hsa-miR-642a-5p, has-miR-141-5pand their target genes predicted by TarBase, respectively. The primary pathway was cytoskeleton actin regulation in a, spliceosome in b and c, NOD-like receptor in d and mRNA surveillance in e signaling pathway. $P \leq 0.05$.

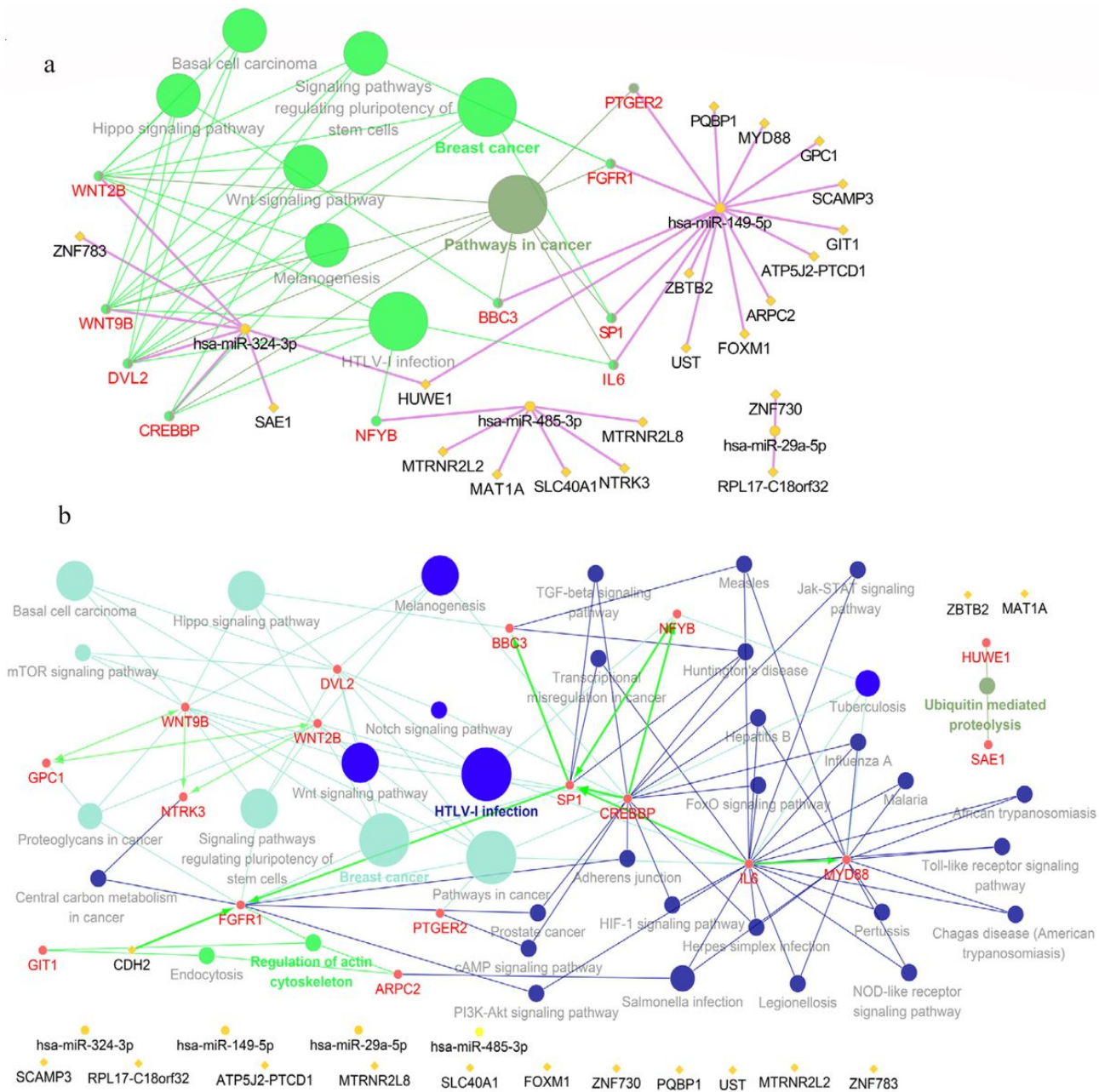


Figure 7

Kyoto Encyclopedia of Genes and Genomes(KEGG) pathway and protein analysis of hsa_circRNA_100375 /hsa-miR-324-3p /hsa-miR-29a-5p /hsa-miR-485-3p /hsa-miR-149-5p axis. A. KEGG pathway showed the axis involved in the cancer-related pathway. B. Certain hub proteins such as FGFR1, PTGER2, WNT9B, WNT2B, SP1, CREBBP, IL-6 and DVL2 played key role in the cancer-related pathway.

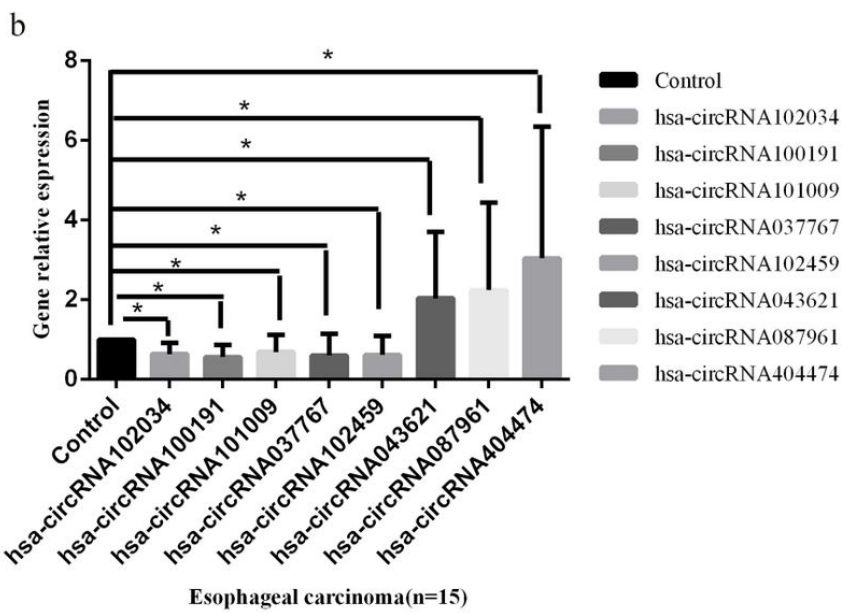
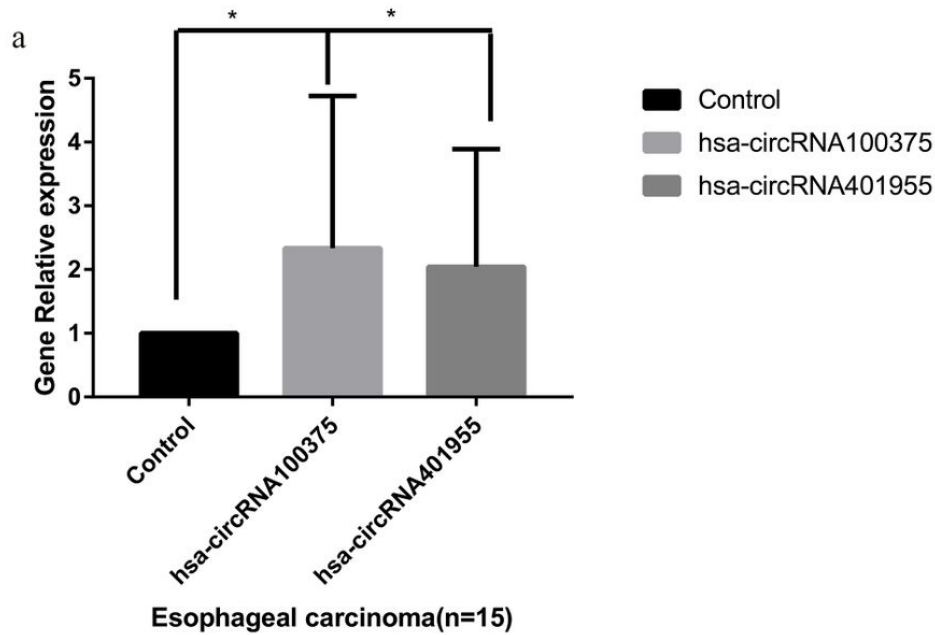


Figure 8

The relative gene expression of most differentially expressed circRNAs (hsa_circRNA_100375, hsa_circRNA_401955, top three upregulated and five downregulated circRNAs). Fifteen patients of esophageal carcinoma were detected by using real-time PCR. The normal adjacent tissue was calculated as the control samples. a: The relative gene expression of hsa_circRNA_100375 and hsa_circRNA_401955. The result showed that the two circRNAs were all significantly decrease in the tumor samples compared to the normal adjacent tissues (*P<0.05). b: The relative gene expression of top three upregulated and five downregulated circRNAs. The result showed that the five downregulated circRNAs (hsa-circRNA102034, hsa-circRNA100191, hsa-circRNA101009, hsa-circRNA037767, and hsa-circRNA102459) were significantly decreased in the tumor tissues, while the top three upregulated circRNAs (hsa-circRNA043621, hsa-circRNA087961 and hsa-circRNA404474) were significantly increased (*P<0.05).